We are IntechOpen,
the world's leading publisher of
Open Access books
Built by scientists, for scientists

4,800
Open access books available

122,000
International authors and editors

135M
Downloads

Our authors are among the

154
Countries delivered to

TOP 1%
most cited scientists

12.2%
Contributors from top 500 universities

CLARIVATE ANALYTICS

BOOK CITATION INDEX

INDEXED

WEB OF SCIENCE™

Selection of our books indexed in the Book Citation Index
in Web of Science™ Core Collection (BKCI)

Interested in publishing with us?
Contact book.department@intechopen.com

Numbers displayed above are based on latest data collected.
For more information visit www.intechopen.com

Self-Assembly of Graphene Nanoribbons Induced by the Carbon Nanotube

Hui Li, Yifan Li and Wei Chen

Additional information is available at the end of the chapter

Abstract

In this chapter, a series of molecular dynamics simulations have been carried out to explore the self-assembly of graphene nanoribbons (GNRs) induced by the single-walled carbon nanotubes (SWCNTs). Simulation results show that GNRs can insert and wrap SWCNTs spontaneously, forming helical configurations and maximizing the π-π stacking area between graphene and SWCNT. The helical configuration takes the least amount of energy and achieves the maximum occupancy. The size and function group of GNR and SWCNT should meet the required conditions to guarantee the self-assembly in insertion and wrapping processes. Several GNRs can spiral in an SWCNT simultaneously, and two formulas have come up in this study to estimate the quantity threshold for multiple GNR spiralling. The rolled GNRs can also spontaneously insert into SWCNTs, forming a DNA-like double helix, or collapsing to a linked double graphitic nanoribbon and wrapping in a helical manner around the tube.

Keywords: molecular dynamics simulation, graphene nanoribbon, structural evolution, helical configuration, self-assembly

1. Introduction

Carbon materials, especially the carbon nanotube and graphene, have attracted tremendous attention on the theoretical research and the potential applications because of their unique configurations and excellent performances. The cylindrical SWCNT possessing a large specific surface area and hollow interior could act as 'molecular straws' capable of absorbing dipolar molecules by capillary action [1]. Over the past decade, the self-assembled systems [2, 3] relied on the special hollow structure of cylindrical SWCNTs, are an attractive class of new bio-inspired nanomaterial for biologists and material scientists, because the self-assembled

materials may not only be designed to be highly dynamic, displaying adaptive and self-healing properties, but could also help gain an understanding of the rules that govern biomolecule assembly processes [4]. In the self-assembly process, the hollow interior of SWCNT can serve as nanometre-sized moulds and templates [5] to control the configuration of other materials, or as a protective layer [6] to prevent the filler from oxidation and shape fragmentation. The physical and chemistry properties of the heterostructure are expected to be modified due to the interaction between SWCNT and exotic materials [7]. Thus, filling SWCNTs with chosen fillers can produce one-dimensional nanostructures with exciting new applications [8]. A wide array of fillers, including various metal atoms [9], halides [10], C60 [11, 12] and polyacetylene [13], were found to be filled into the SWCNT, with novel configurations and properties. Strano et al. [14] found that water molecules displayed different phase transition temperatures when confined in the nanotube. C60 [15] or other spherical metallofullerenes [16] were distributed evenly along the axial direction after self-assembling into the SWCNT just as beans distributed in pod, while those linear fillers such as DNA [17] and polyacetylene [13] were easy to insert into or wrap the SWCNT spontaneously with an interesting helical configuration.

Recently, our studies [18, 19] indicated that GNRs, the material with unique optical, magnetic and electrical properties [20–23], have been succeeded in spontaneously and spirally wrapping and inserting into the SWCNT. GNRs possess intriguing electronic structures ranging from semiconducting to half-metallic, depending on their geometry and dimensions. Thus, the helical composite structures formed by two novel carbon materials are expected to have excellent properties, such as high carrier mobility and high mechanical strength, to be used in microcircuit interconnectors, nanoelectronic devices and nanosensors [24–26]. And a convincing model on the interaction between the GNR and SWCNT may inspire great efforts in theoretical studies, synthesis and chemical modifications which focus on their electronic, biological, chemical and even magnetic properties. In this chapter, the self-assembly behaviour of GNRs, especially multiple GNRs, induced by SWCNT is studied in detail, while the mechanism and influencing factors of self-assembly are also described, providing an opportunity for a comprehensive and satisfactory understanding of how to control the composite structure of this SWCNT-GNR nanomaterial hybrid. This discovery is of great significance in the exploration of the properties of the GNR-SWCNT system and may expand the applications of GNR and SWCNT in extensive fields involving medicine, chemistry, biology and even fuel cells. The perfect GNR helix in SWCNT may be used to control the band gap of various GNT-based nanodevices, which will pave the way for the progress of nanoelectronics.

2. Simulation method

Molecular dynamics method is used to study the self-assembly behaviour of GNRs induced by SWCNTs. The force field of condensed-phase optimized molecular potentials for atomistic simulation studies (COMPASS) [27] is applied to model the atomic interaction. COMPASS is an ab initio force field which has been parameterized and validated using

condensed-phase properties, various ab initio calculations and experimental data, with a functional form that includes covalent terms, van der Waals interactions and electrostatic forces. The aim of the force field is to achieve high accuracy in predicting the properties of complex mixtures [28] and it has been widely used due to its potential to obtain reasonable results in terms of the mechanical properties of CNTs [29, 30]. The van der Waals energy is described by LJ-96 function [28] in COMPASS force field, the functional forms of which is listed as: $E = D_0 \left[2 \left(\frac{R}{R} \right)^9 - 3 \left(\frac{R}{R} \right)^6 \right]$, where D_0 = 0.064 Kal/mol and R_0 = 4.01Å [31, 32]. The temperature in this paper is chosen as 298 K in the NVT canonical ensemble (number of particles, volume and temperature are constant). Andersen thermostat [33] is employed to control the thermodynamic temperature and generate the correct statistical ensemble by allowing the simulated system to exchange energy with a 'heating bath'. The speed of atoms follows the Maxwell-Boltzmann distribution and the time integration is undertaken using the velocity Verlet algorithm. The simulation time step is 1.0 fs. Each system is simulated for sufficient time to reach equilibrium. Trajectory is recorded every 5.0 ps for further analysis. The GNR with the opening edge is prepared by cutting the parallel sheet of block graphite.

3. Helical insertion of GNRs

Direct simulations in **Figure 1(a)** show the self-assembly of six GNRs into the fixed SWCNT. The length of SWCNTs is 98.38Å and six GNRs have the same size of 5.681Å in width and 147.600Å in length. When one end of the GNR is captured by the SWCNT, the GNR adheres onto the tube wall parallel and moves towards the tube. At the beginning, six GNRs fill into the cavity of SWCNT synchronously and spontaneously under the action of van der Waals coupling. When the simulation time is up to 2.3 ns, a clear and symmetrical multiple helical configuration with uniform pitch is formed in SWCNT, like an upgrade of the double helix of DNA [34] or the triple helix of collagen [35] in biology, suggesting nature's preference for helical structure. While the processes of encapsulating and spiralling are terminated, no more axial movement of the helical GNRs has been observed due to the van der Waals potential well, but rotation is continued in their circumferential direction, resulting the GNR tails outside SWCNT keeps a new subtle spiral morphology by movement inertia. In addition, for the helical GNRs in SWCNT, the essential corrugation [36] is suppressed by the enhanced interaction between GNRs and SWCNT, inspiring an efficient way to straighten the twisted and corrugated GNRs. The filling snapshots of six GNRs into the unfixed SWCNT are established in **Figure 1(b)** where a slight deformation of carbon nanotube appears followed by the formation of a perfect single helix of GNRs at 0.95 ns. The unfixed SWCNT-GNR system takes shorter time to attain equilibrium, demonstrating that the deformation and movement of carbon nanotubes do not hinder the self-assembly of GNRs, but improve their filling speed.

To further research the helical configuration of the multiple GNRs self-assembled into SWCNT, different numbers of annular and multilayer GNRs filling into SWCNT are shown in **Figure 2**. For convenience, a new and canonical definition for $(a_1, a_2 \ldots a_i \ldots a_N)$ and $[a_1, a_2 \ldots a_i \ldots a_N]$ is set, where a_i means the number of GNRs in i-layer and parentheses and square brackets refer to the simulated model and result, respectively. **Figure 2** illustrates that different numbers of GNRs can

self-assemble into SWCNTs to form different layers of helical structures. As shown in **Figure 2(a)**, seven GNRs self-assemble and form a monolayer helical configuration in SWCNT, while for the system of eight GNRs, a GNR deviates from the first helix into the second one in **Figure 2(b)**, suggesting that there is a quantity threshold for every GNR helix. The helical angle of inner GNRs is easily affected by the outer one to ensure the maximum overlap between GNRs in different helices when few GNRs in the inner helix are located, as the royal blue GNR in **Figure 2(b)**. But when several GNRs locate on the inner helix (**Figure 2(c)**), their helical angle does not easily affect each other. This phenomenon might be useful when adjusting or controlling the self-assembly morphology of GNRs in SWCNT. Another noteworthy phenomenon is that the outer GNRs can enter the inner layer spontaneously in **Figure 2(d)** and **(e)**, which is closely related to the self-assembly mechanism of GNRs and is explained in detail in Section 4. When encapsulating the (7, 4, 2) GNRs into SWCNT in **Figure 2(f)**, the GNRs arrange densely to obtain a perfect multiple spiral structure, and no GNR transfers into the inner helix. When setting more GNRs in SWCNT like in **Figure 2(g)** and **(h)**, the self-assembly process also exists but the helical configuration becomes imperfect due to their undistinguished layer. In addition, the well-organized spiral configuration of (7, 4, 2) consists of an array of helicoids formed concentrically (shown in **Figure 2(j)**), similar to the stranded wire in cable (shown in **Figure 2(k)**), so the GNR@SWCNT composite structure could be expected to have excellent performance in mechanics and electrics like stranded wire.
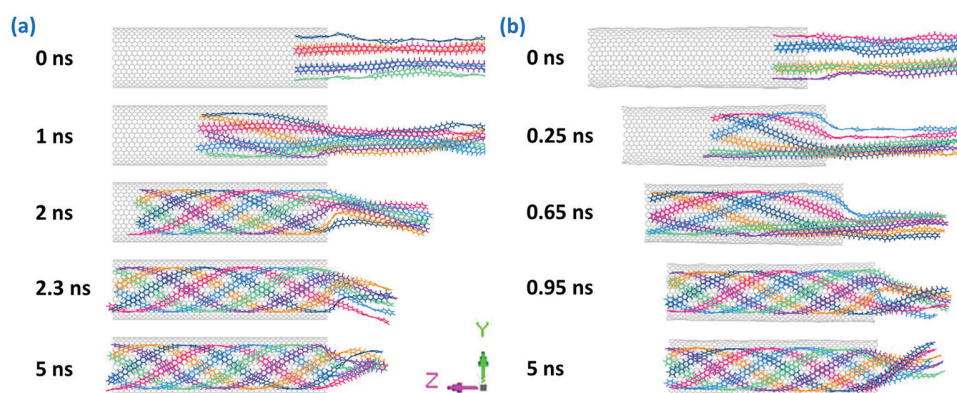

Figure 1. The insertion and helix-forming process of six GNRs into SWCNT: (a) snapshots of GNRs encapsulated in the fixed SWCNT; (b) snapshots of GNRs encapsulated in the unfixed SWCNT.

The rolled GNR, which is obtained by connecting the two ends of straight GNR, can also self-assemble into SWCNT to form a double-helical configuration. **Figure 3(a)** provides the representative snapshots of a rolled GNR inserted helically into the SWCNT. At the beginning, a rolled GNR is placed near the SWCNT separated by 5Å. As time continues, the rolled GNR tends to be collapsed. Due to the Van der Waals force [37] between the rolled GNR and SWCNT, the rolled GNR stretches its cross section and is close to the SWCNT at 0.1 ns. Then, the portion of the rolled GNR near the entrance is captured by the SWCNT hollow space and starts to move forward along the inner wall of the SWCNT. After an initial correlation time, the rolled GNR begins to curl in the SWCNT (at t = 3.5 ns). When the simulation time reaches 4.8 ns, the rolled GNR shows a clear helical conformation with a large pitch. Then, the helix becomes denser to occupy the entirety of the tubes. Eventually, a perfect DNA-like

double-helix configuration with remarkably constant pitches is formed in the SWCNT. The result of two rolled GNRs self-assembling into the SWCNT is shown in **Figure 3(b)**. The two rolled GNRs with the same length are placed at the two ends of the SWCNT. When the simulation begins, the two rolled GNRs are captured by the inner hollow of the SWCNT simultaneously. After they contact with each other, one of them is pushed down to a two-layer graphitic nanoribbon, and then spirals like an unrolled GNR. As the simulation time reaches 2.25 ns, helices arise at both of the rolled GNRs. At the simulation time of 5.0 ns, the two rolled GNRs display a clear helical conformation.
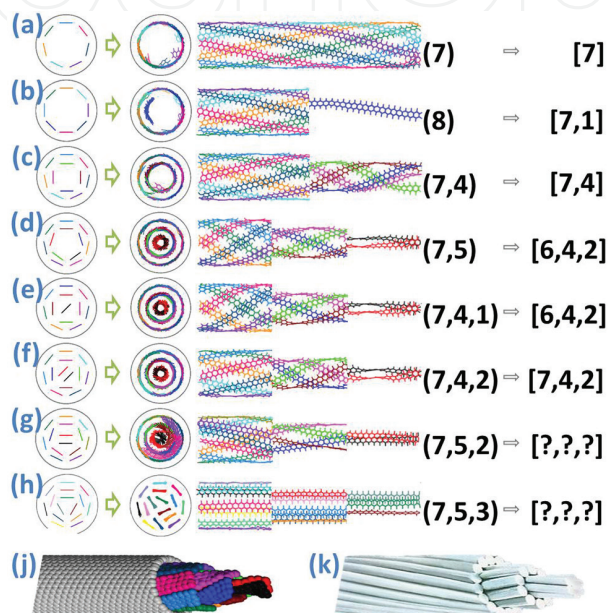
Figure 2. The initial arrangement and equilibrium configuration of the annular and multilayer GNRs in SWCNT. From (a) to (h), the number of GNRs is 7, 8, 11, 12, 12, 13, 14 and 15, respectively; (j) Corey-Pauling-Koltun configuration of the (7, 4, 2) GNRs; and (k) configuration of the stranded conductor in cable.
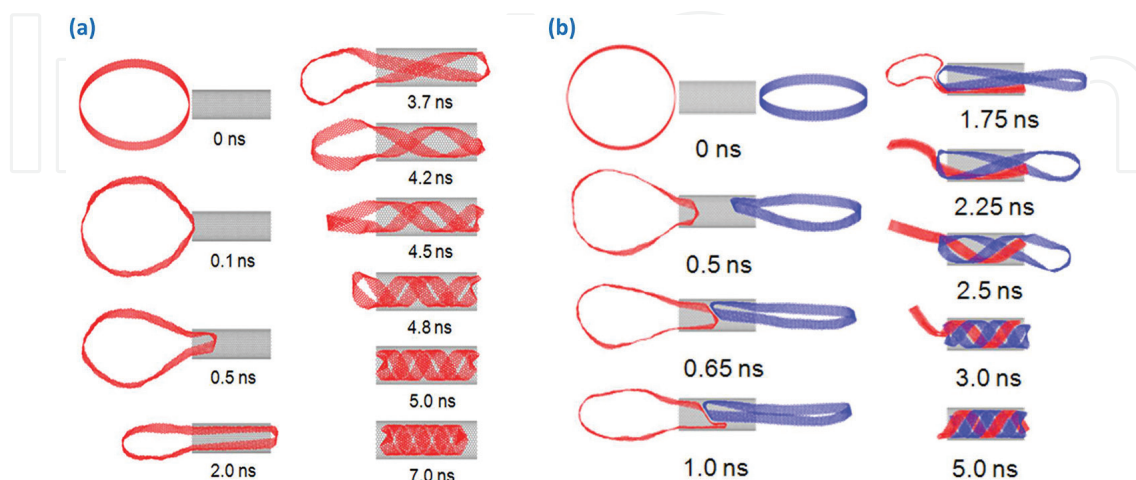

Figure 3. Representative snapshots of (a) a rolled GNR and (b) two rolled GNRs self-assembling into the SWCNT to form helical configurations. The length of the GNR is 46.40Å.

4. Interaction mechanism

Why the GNR could self-assemble into the SWCNT and develop a helical manner? To further study its interaction mechanism, the final geometric configuration and energy evolution of this self-assembly system are displayed in this section.

Figure 4 shows the concentration distribution profile of the multiple-layered GNR@SWCNT system to help characterize the parameters of the multiple helical configurations. Although the peak of concentration distribution profiles is split near the centre of SWCNT due to the rigidity of C-C bond and the larger curvature in the inner helix, it can be measured that the separation of the adjacent layers is 3.5Å, similar to the basal plane separation in graphite or the wall thickness of the multi-walled carbon nanotubes (3.4Å). That is to say, GNRs are arranged very closely in the limited space of SWCNTs. In the crowded environment, long molecular chains frequently adopt ordered, helical conformations, which has been confirmed by Snir and Kamien [38]. In their simulation system, a solid, impenetrable but flexible tube was immersed into a solution of hard spheres. It is amazing that the flexible tube will take on a regular helical configuration which takes up the least space. The enlarged environment entropy is considered to be the driving force of helix formation.
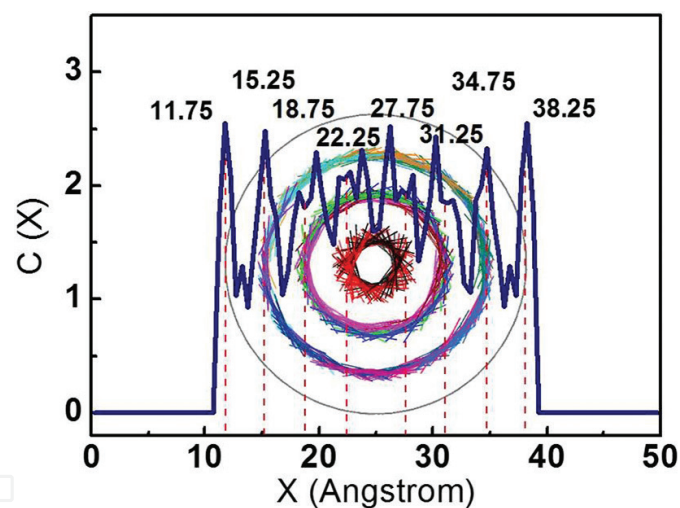
Figure 4. Concentration distribution profiles of the GNR and SWCNT in the (7, 4, 2) system in the X-direction.

On the other hand, the spontaneous filling and intertangling of GNRs are also driven by the increasing π-π stacking area between GNRs and SWCNT, because the system energy is released when carbon six-membered rings are stacked. In order to confirm this view, a series of simulations about different SWCNTs are studied. **Figure 5(a)** shows that similar multiple helical configurations are taken in cylindrical SWCNT shell to maximize their π-π stacking area, while the flat GNRs are obtained in the special cubical fixed SWCNT because this configuration can guarantee the largest stacking area with the straight and stationary tube wall. The partial enlarged view of the GNR@SWCNT helical configuration is displayed in **Figure 5(b)**, demonstrating that the GNR ring is offset from SWCNT ring slightly and their centroid-centroid distance is 3.858Å, consistent with the typical aromatic-aromatic offset π-π stacking [39].
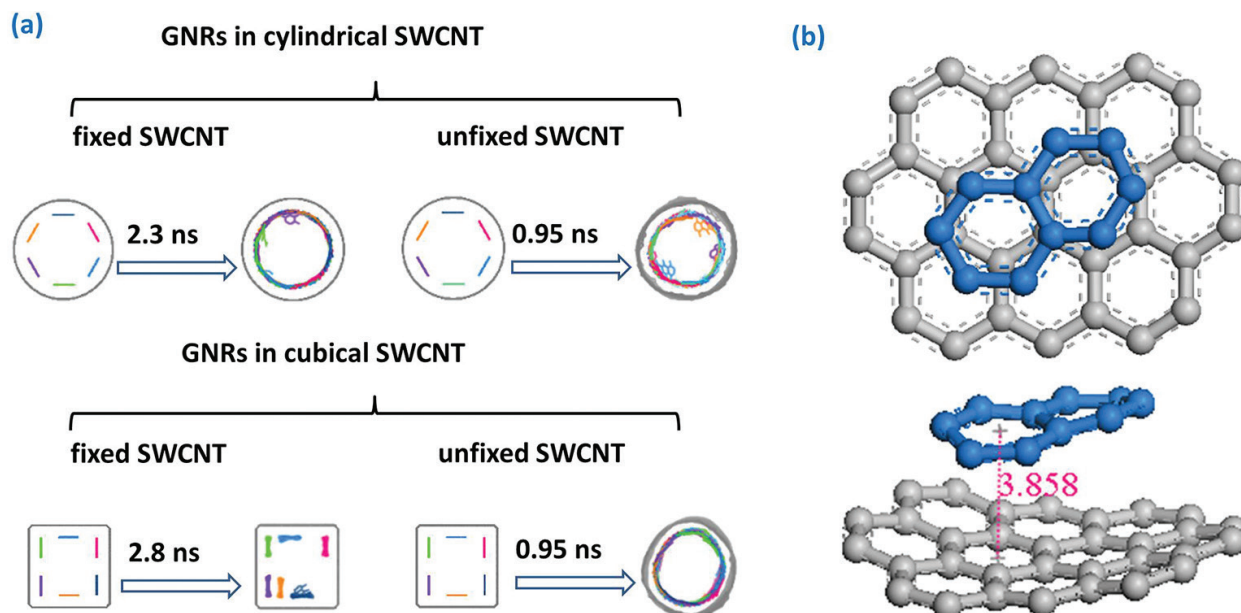
Figure 5. (a) The effect of the SWCNT configurations on the self-assembly process and (b) partial enlarged detail of the GNR@SWCNT helical configuration where SWCNT is grey and GNR is blue.

Figure 6 illustrates the potential energy (E_p), van der Waals interaction energy (E_{vdw}) and π-π stacking area for the GNR@SWCNT system as functions of simulation time in the self-assembly process. The evolution of π-π stacking area and system energy is identical, demonstrating that the energy decreasing is caused by the π-π stacking area expanding and the van der Waals interaction between the GNRs and SWCNT plays a dominant role in driving the formation of the helical configuration. The decline of potential energy indicates that the self-assembly course is spontaneous. Taking the self-assembly of (7, 4, 1) GNRs as an example, a clear change of energy gradient is shown in **Figure 6(a)**. The initial large energy gradient is contributed by the rapid expansion of π-π stacking areas as multiple GNRs filling into SWCNT. Then, the energy gradient decreases when the GNRs reach the other end of the carbon nanotube, because the tail of GNRs inserts into the SWCNT slowly with GNRs spiralling and configuration optimizing. As for the (7, 4, 1) GNRs in **Figure 6(b)**, both energy curves are divided into two stages, corresponding to two processes of structural changing. In the first stage from 0 to 1.8 ns, multiple GNRs encapsulate into carbon nanotube along their original directions and remain stable for some time. Then in the second stage (2.3–2.6 ns), two GNRs transfer into inner helical structure individually from the first and the second helix to obtain the largest π-π stacking area for the system, so the system configuration is changed from the (7, 4, 1) to (6, 4, 2) with a rapid decrease of potential energy, suggesting that this process can improve their stability. In this process, the van der Waals energy drops 0.7 Mcal/mol and the potential energy drops just 0.5 Mcal/mol, indicating that the disappeared energy is stored efficiently by the bending of new inner GNRs.

In principle, the helical self-assembly is determined by the competition between the van der Waals energy and the bending strain energy of GNRs [40]. The former provides an attractive force to spiral GNRs, and the latter usually tends to maintain the GNRs in their original form [41]. During the self-assembly process, the van der Waals interaction helps the GNRs

overcome their energy barrier caused by the bending strain energy, and drives the GNRs to be trapped in the SWCNT and undergo self-scrolling. Throughout the helix-forming course, the van der Waals energy has partially converted into the internal energy of GNRs for their mechanical deformation and partially converted into kinetic energy.
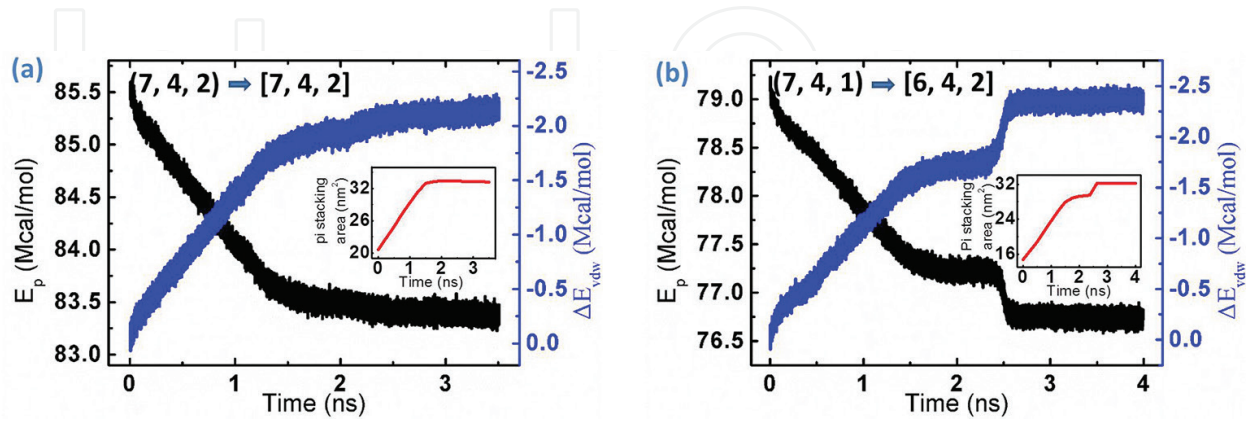
Figure 6. The potential energy (E_p) of GNR@SWCNT system and the van der Waals interaction energy (E_{vdw}) between the GNR and SWCNT as functions of simulation time in the helical encapsulation of (a)13 GNRs and (b)12 GNRs, and the inserted graph is the corresponding evolution of π-π stacking area.

## 5. Dependence of size, function group and initial arrangement of GNRs

In order to further exploit the effect of system size on self-assembly, a series of simulations and parameter analyses have been completed. **Figure 7** reveals that all GNRs of different widths in the SWCNT of different diameters are able to form the perfect helical structures, with varying screw pitches. The helical angle increases with GNR width but have no clear monotone change tendency with SWCNT diameter. In the self-assembly process, more time is needed to form a large helical angle because of the sluggish motion and coordination of multiple GNRs. Besides, the relation between system size and threshold value is also shown in **Figure 7**. It can be seen that the simulated threshold of GNRs in the first perfect helix is inverse with their width due to the limited space inside SWCNT but has a positive correlation with SWCNT diameter.

A simple mathematical model (**Figure 8**) is built to calculate the quantity threshold for the helical GNRs self-assembled in SWCNT. Three formulas are given as follows.

The threshold of GNRs in i-layer is

$$V_i = \left\lfloor \frac{(D - 2iA)\pi}{A' + W} \right\rfloor \tag{1}$$

where D is the SWCNT diameter, i is the sequence of the GNR helix, A is the fixed distance between GNRs and SWCNT, A' is the fixed distance between adjacent turns of GNRs and W is the GNR width. The specific square brackets mean that the calculated value should be rounded down to the nearest whole unit. All distances are in units of Angstroms.
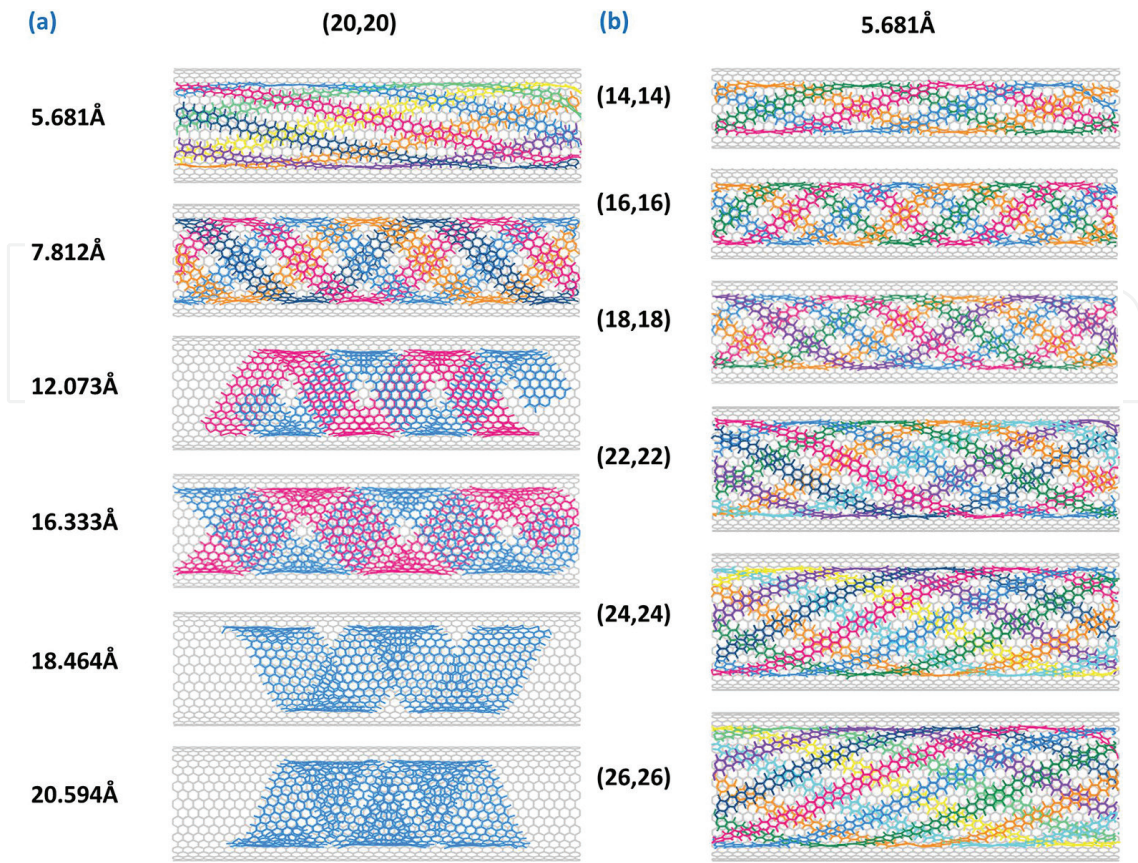
Figure 7. The dependence of the diameter of SWCNT and the width of GNRs in the evolution: (a) helical encapsulation of GNRs with different width into the SWCNT (20, 20); (b) helical encapsulation of GNR into the SWCNT with different diameter.
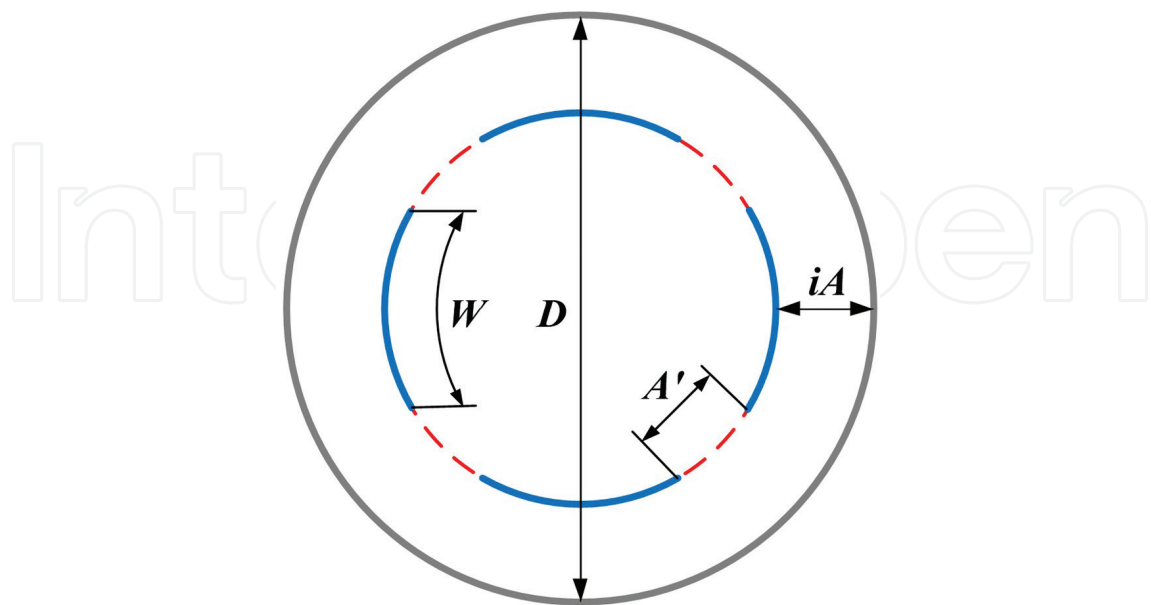
Figure 8. The ideal model of the cross section of GNR@SWCNT helical structure. SWCNT and GNR are referred to as grey circle and blue arc, respectively.

The whole threshold of the self-assembly system is

$$V_{total} = \sum_{i=1}^{N} V_i \qquad (2)$$

where N is the number of GNR helix in SWCNT, which is described by

$$N = \left\lfloor \frac{D}{2A} \right\rfloor \qquad (3)$$

The above formulas are used to calculate the theoretical threshold for 5.681Å GNR in (20, 20) SWCNT, and the result is consistent with the acquired thresholds of the first, second GNR helix and whole system very well. So the formulas are proved applicable to estimate the quantity threshold for the helical GNR in SWCNT.

Then, the effect of system size on the self-assembly of rolled GNRs is further studied. **Figure 9(a)** shows the diameter threshold of SWCNT which could be successfully encapsulated by the rolled GNRs with certain widths. It can be observed that the SWCNT diameter should be larger than the threshold to ensure the collapse and insertion of the rolled GNR. When the SWCNT diameter is too small, the van der Waals interaction cannot overcome the large energy barrier in system and the distance between GNR and SWCNT cannot maintain 3.5Å due to the confinement. Consequently, the SWCNT size should be chosen appropriately according to the GNR width to facilitate the self-assembly. In addition, **Figure 9(b)** demonstrates that a perfect helix inside the nanotube can be obtained when the space inside the nanotube is sufficient, which is independent of the diameter of the SWCNT. But what would happen if the length of the SWCNT is too short? **Figure 9(c)** shows the snapshots of the rolled GNR self-assembling into the short SWCNT. The rolled GNR inserts into the SWCNT successfully with the trapped portion to form a helix. After the helical configuration in SWCNT is closely packed, the front helical GNR is pushed out and the GNR tail continuously enters the SWCNT in a helical manner. Finally, the rolled GNR attempts to be symmetric to the tube, with the middle GNR in the short SWCNT forming a perfect helical configuration.
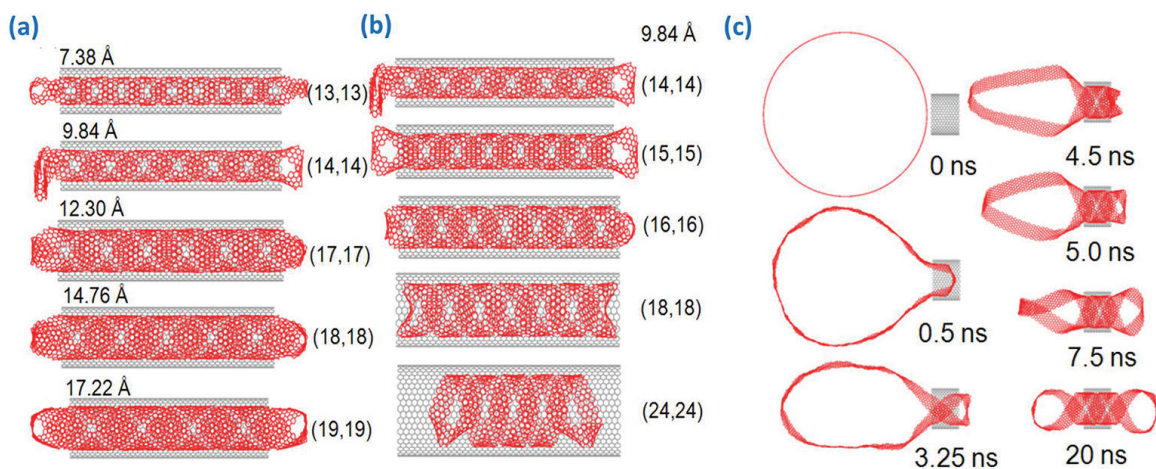
Figure 9. (a) The critical diameters of the SWCNTs to guarantee the insertion of the rolled GNR with different widths successfully: GNR(7.38Å)@SWCNT (13,13), GNR(9.84Å)@SWCNT (14,14), GNR(12.30Å)@SWCNT (17,17), GNR(14.76Å)@SWCNT (18,18), GNR(17.22Å)@SWCNT (19,19), respectively. (b) The helical insertion of GNR with the width of 9.84Å into the SWCNT with different diameters. (c) Representative snapshots of a rolled GNR inserting into the SWCNT (25, 25) with the length of 24.60Å to form a helical configuration.

The self-assembly of GNRs into SWCNT can be utilized to deliver substances into the nanoscale-confined space without any other external force. In order to explore its possible applications, different functional groups are modified on the edge of the rolled GNR. As shown in **Figure 10(a)**, the rolled GNR modified with 133 –OH can self-assemble into the SWCNT spontaneously to form a helix, and the interval between neighbouring segments is proved to be influenced by the chemical groups –OH. Then, a series of simulations are performed on the rolled GNR that is modified with different number of –OH, as shown in **Figure 10(b)**. The results demonstrate that the rolled GNR can form a helix in the SWCNT when one end of the GNR is modified with 50,100 and 133 –OH. By contrast, the rolled GNR cannot form a helix when fully modified with 200 –OH at one end, and even cannot be trapped by the hollow interior of the SWCNT when modified with 400 –OH. Another functional group, the –H, is also chemically attached to the rolled GNR uniformly. When the dangling σ-orbitals on the GNR are all saturated by hydrogen atoms, the rolled GNR can still self-assemble into the SWCNT and form a helix, which is quite different from the result of the GNR modified with –OH, indicating that the functional groups on the GNRs have a significant influence on their self-assembly. In addition, the spiral of the GNR without any dangling σ-orbitals also reveals that the van der Waals interaction is the main driving force of the helix self-assembly, rather than the dangling σ-orbitals at the edge of GNRs [42]. At the same time, the stability of the final configuration in different systems has been verified. **Figure 10(c)** shows that the potential energy of the 200 –OH system decreases to a certain value and then maintains at this level for 7 ns, indicating that the non-helical configuration is comparably stable. The potential energy in the system of GNR modified with 133 –OH is very different (**Figure 10(d)**) as it is divided into several periods: two 'rapid drop' periods, a 'platform' period and an equilibrium state. So it may be suspected that the modification of the GNR with different functional groups can influence the final configuration of the GNR@SWCNT system.

In addition, we further simulate the influence of the temperature on the final structure of the GNR@SWCNT system. It is surprising that the final composite structure of the GNR@SWCNT system can maintain stability even when the temperature is 1000 K.
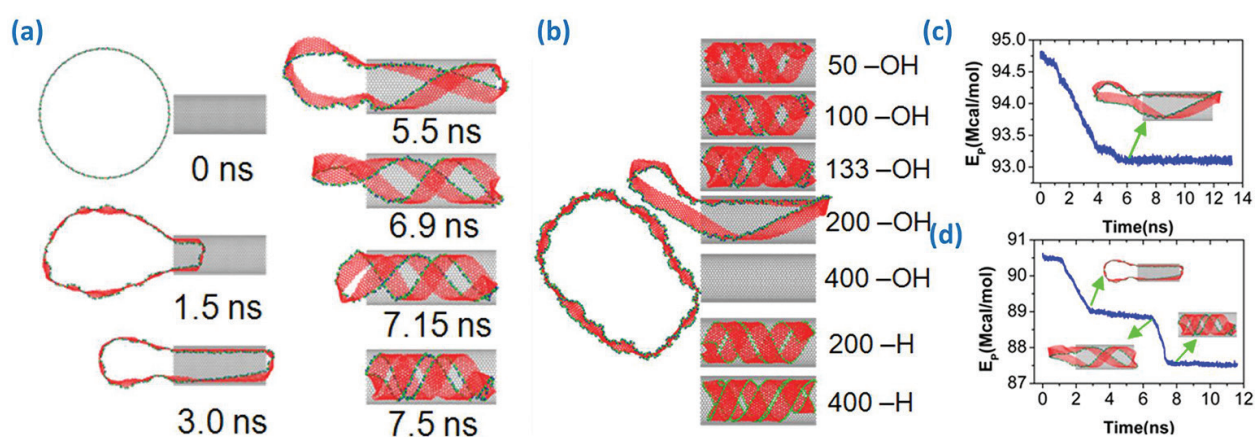

Figure 10. (a) Self-assembly snapshots of the GNR modified with –OH entering with the SWCNT (30, 30). The length of the GNR is 135.6Å, the width of the GNR is 14.76Å and the number of the –OH is 133. (b) Final configuration of this GNR modified with functional groups encapsulated into the SWCNT (30, 30). Total potential energy (E_P) of the GNR-SWCNT systems as functions of time: (c) the GNR modified with 200 –OH and (d) the GNR modified with 133 –OH.

6. Helical wrapping of GNRs

The above studies mainly focus on the insertion of GNRs into the hollow SWCNTs, but there is another form of self-assembly for the GNR/SWCNT system. This section investigates the collapse and wrapping characteristic of the rolled GNRs around the SWCNT. **Figure 11(a)** shows the typical snapshots of the rolled GNR spontaneously wrapping on the SWCNT (15, 15). Initially, the circular rolled GNR is positioned in the centre of the SWCNT, with the axis parallel to the SWCNT and the offset distance of about 5Å above the SWCNT. As shown in **Figure 11(a)**, the rolled GNR approaches the SWCNT rapidly due to the strong attractive force between them. During the approaching process, the rolled GNR stretches its cross section from a circle to an oval gradually because the carbon atoms close to the SWCNT endure stronger van der Waals force than the uppers. When the lower atoms in rolled GNR come into contact with the SWCNT, the upper atoms continue approaching the SWCNT, inducing the oval cross-section collapses to a triangle one [43] that could cover the upper surface of the SWCNT completely. Then the GNR rotates and its cross section changes into a bow shape in 5.5 ns. During the above process, the rolled GNR collapses rather slowly because the van der Waals interaction on the top semi-circular tube is so weak. But when th'e simulation reaches 9 ns, the collapse of the entire rolled GNR is further accelerated due to the increasing contact area [40] between SWCNT and GNR. The sequential collapse of these rings manufactures a linked double-layered GNR and then results in a double-walled helix wrapping around the SWCNT with a large helical pitch. Regardless of the angle between the two axes of the rolled GNR and SWCNT, the GNR can wrap around the SWCNT helically. The GNR helix out of the SWCNT wall is similar to the tendril of a morning glory climbing around a tree trunk where growth pattern helps the plant to maximize the sunlight absorption in the minimum space and grow strong. **Figure 11(b)** and **(c)** shows the concentration distribution profiles of the final configuration in the X-direction and the total potential energy of the GNR/SWCNT system in the wrapping process. The former figure reveals that the distance between two layers of the CNR outside the tube is also about 3.5Å, and the latter energy curve has a decreasing tendency with the simulation time and finally reaches the minimum at equilibrium, similar to the insertion of GNRs into SWCNT, meaning that the wrapping self-assembly of GNR/SWCNT has the same mechanism as the filling self-assembly.

The different final configurations of the rolled GNRs adhering on the SWCNTs are summarized in **Figure 12**. The length of all SWCNTs (15, 15) is 73.79Å, and the width of all rolled GNRs is 14.76Å. All rolled GNRs are circular initially. As illustrated in **Figure 12**, the rolled GNRs with a length larger than the threshold of 38.33Å are collapsed. However, the rolled GNRs with diameters between 157.61 and 230.03Å cannot fully collapse, but simply deform from cylindrical symmetry to bow shapes, which is because the van der Waals interaction in these system cannot overcome the energy required for the fully mechanical deformation of the round GNRs, leading to the mechanically bistable configuration [41]. When the GNR length continues to increase more than 234.30Å, the perfect helix outside of SWCNT can be guaranteed.
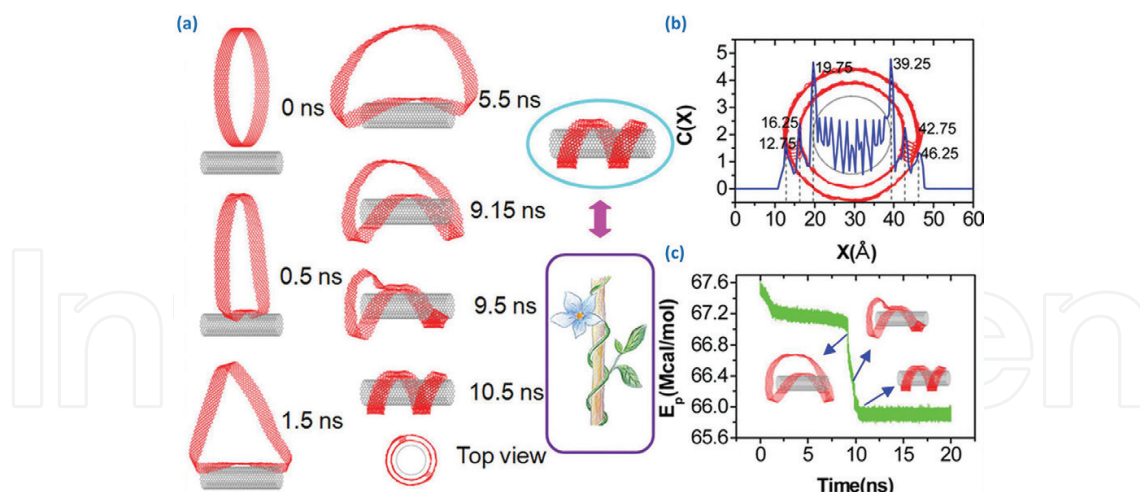
Figure 11. (a) Representative snapshots of a rolled GNR wrapping on the SWCNT (15,15) to form a spiral configuration, which resembles the tendril climbing around a trunk (hand drawn sketches by Wei Chen). The width of the GNR is 14.76Å and the length of the SWCNT is 73.79Å. (b) Concentration distribution profiles of the GNR and SWCNT in the system in the X-direction. (c) Total potential energy (E_p) of the GNR-SWCNT systems as a function of time.

Length of GNR	Final configuration	Representive snapshots	Conclusion (L: length)
25.57	●		
29.81	●		Uncollapsed: L≤34.09Å
34.09	●		
38.33	▲		
46.87	▲		Full-collapsed:
63.90	▲		34.09Å≤ L≤153.37Å
127.80	▲		
136.31	▲		
153.37	▲		
157.61	★		
170.40	★		
191.70	★		Semi-collapsed:
213.00	★		153.37Å≤ L≤230.03Å
225.79	★		
230.03	★		
234.30	■		
247.09	■		Helical configuration:
255.60	■		L≥230.03Å
340.80	■		

● stands for circle configuration without collapse;
▲ stands for the full-collapse parallel to the axe of the nanotube;
★ stands for the semi-collapse;
■ stands for the full-collapse to form a helical configuration.

Figure 12. The final configuration of rolled GNRs with different lengths adhering on the SWCNT (15, 15). The width of the GNRs is 14.76Å and the length of SWCNTs is 73.79Å.

7. Conclusion

In summary, this work proves that the multiple and rolled GNRs can self-assemble into or wrap around the cylindrical SWCNT to form a well-organized multiple helical configuration which takes the least amount of energy and takes up the least space. The self-assembly process is driven by the van der Waals interaction between the GNRs and the SWCNT, because this energy is released when carbon six-membered rings are stacked. The final self-assembly configuration of GNRs is responsible for the combined effect of system size and functional groups. The sizes of the SWCNTs should exceed a certain value to ensure the insertion of GNRs with certain widths, while they have negligible effects on the formation of the perfect helix after GNR encapsulation. The quantity threshold of GNRs inside SWCNT increases with the SWCNT diameter and decreases with the GNR width, and it can be estimated by the empirical formulas shown in this paper. The modification on GNR edge can influence the final configuration in the self-assembly process. In addition, the results of this study also reveal that the size of GNRs and SWCNTs should meet some required conditions to guarantee the wrapping self-assembly outside of the SWCNT in a helical form.

The helical configuration of the GNRs is similar to the ordered, spiral structure of long molecular chains such as DNA and protein in the confined cell. In fact, the spiral phenomenon is common but interesting in the nature, such as the spiral arrangement of florets in sunflower, the spiral nucleation of SiC crystal in a limited space and the spiral air flow in the centre of a tropical cyclone. What's more, Chinese old Tai Chi totem also emphasizes the philosophy of helical configuration, which implies that the universe derives from a series of helix. Thus, the findings in this paper are of great importance towards the better understanding of the helix, and of significance in predicting and controlling the self-assembly configuration. Moreover, the unique phenomenon of self-assembly in the GNRs/SWCNT system has potential advantages in the application as nanocontainer for drug delivery and molecular transportation. And this composite structure can also be used to fabricate functional nanodevices, such as sensor, nanoelectronic components, integrated circuits and optoelectronic devices.

Acknowledgements

Author details

Hui Li*, Yifan Li and Wei Chen

*Address all correspondence to: lihuilmy@hotmail.com

Key Laboratory for Liquid-Solid Structural Evolution and Processing of Materials, Ministry of Education, Shandong University, Jinan, People's Republic of China

References

[1] Pederson MR, Broughton JQ. Nanocapillarity in fullerene tubules. Physical Review Letters. 1992;**69**(18):2689–92. doi:10.1103/PhysRevLett.69.2689

[2] Serpell CJ, Rutte RN, Geraki K, Pach E, Martincic M, Kierkowicz M, et al. Carbon nanotubes allow capture of krypton, barium and lead for multichannel biological X-ray fluorescence imaging. Nature Communications. 2016;**7**:13118. doi:10.1038/ncomms13118

[3] You Y, Wei R, Yang R, Yang W, Hua X, Liu X. Crystallization behaviors of polyarylene ether nitrile filled in multi-walled carbon nanotubes. RSC Advances. 2016;**6**(75):70877–83. doi:10.1039/C6RA11783J

[4] Sadownik JW, Ulijn RV. Dynamic covalent chemistry in aid of peptide self-assembly. Current Opinion in Biotechnology. 2010;**21**(4):401–11. doi:10.1016/j.copbio.2010.05.010

[5] Nakanishi R, Kitaura R, Warner JH, Yamamoto Y, Arai S, Miyata Y, et al. Thin single-wall BN-nanotubes formed inside carbon nanotubes. Scientific Reports. 2013;**3**:1385. doi:10.1038/srep01385

[6] Choi WY, Kang JW, Hwang HJ. Structures of ultrathin copper nanowires encapsulated in carbon nanotubes. Physical Review B. 2003;**68**(19):193405. doi:10.1103/PhysRevB.68.193405

[7] Shao J, Yang C, Zhu X, Lu X. Melting and freezing of Au nanoparticles confined in armchair single-walled carbon nanotubes. The Journal of Physical Chemistry C. 2010;**114**(7):2896–902. doi:10.1021/jp910289c

[8] Gately RD, in het Panhuis M. Filling of carbon nanotubes and nanofibres. Beilstein Journal of Nanotechnology. 2015;**6**:508–16. doi:10.3762/bjnano.6.53

[9] Sun FW, Li H, Liew KM. Compressive mechanical properties of carbon nanotubes encapsulating helical copper nanowires. Carbon. 2010;**48**(5):1586–91. doi:10.1016/j.carbon.2009.12.056

[10] Nie C, Galibert A-M, Soula B, Flahaut E, Sloan J, Monthioux M. A new insight on the mechanisms of filling closed carbon nanotubes with molten metal iodides. Carbon. 2016;**110**:48–50. doi:10.1016/j.carbon.2016.09.001

[11] Hirahara K, Bandow S, Suenaga K, Kato H, Okazaki T, Shinohara H, et al. Electron diffraction study of one-dimensional crystals of fullerenes. Physical Review B. 2001;**64**(11):115420. doi:10.1103/PhysRevB.64.115420

[12] Farimani AB, Heiranian M, Aluru NR. Nano-electro-mechanical pump: Giant pumping of water in carbon nanotubes. Scientific Reports. 2016;**6**:26211. doi:10.1038/srep26211

[13] Lv C, Xue Q, Shan M, Jing N, Ling C, Zhou X, et al. Self-assembly of double helical nanostructures inside carbon nanotubes. Nanoscale. 2013;**5**(10):4191–9. doi:10.1039/c2nr33157h

[14] Agrawal KV, Shimizu S, Drahushuk LW, Kilcoyne D, Strano MS. Observation of extreme phase transition temperatures of water confined inside isolated carbon nanotubes. Nature Nanotechnology. Forthcoming. doi:10.1038/nnano.2016.254

[15] Smith BW, Luzzi DE. Formation mechanism of fullerene peapods and coaxial tubes: A path to large scale synthesis. Chemical Physics Letters. 2000;**321**(1–2):169–74. doi:10.1016/S0009-2614(00)00307-9

[16] Sato Y, Suenaga K, Okubo S, Okazaki T, Iijima S. Structures of D5d-C80 and Ih-Er3N@C80 fullerenes and their rotation inside carbon nanotubes demonstrated by aberration-corrected electron microscopy. Nano Letters. 2007;**7**(12):3704–8. doi:10.1021/nl0720152

[17] Caoduro C, Hervouet E, Girard-Thernier C, Gharbi T, Boulahdour H, Delage-Mourroux R, et al. Carbon nanotubes as gene carriers: Focus on internalization pathways related to functionalization and properties. Acta Biomaterialia. 2017;**49**:36-44. doi:10.1016/j.actbio.2016.11.013

[18] Li Y, Chen W, Ren H, Zhou X, Li H. Multiple helical configuration and quantity threshold of graphene nanoribbons inside a single-walled carbon nanotube. Scientific Reports. 2015;**5**:13741. doi:10.1038/srep13741

[19] Chen W, Li H. How does carbon nanoring deform to spiral induced by carbon nanotube? Scientific Reports. 2014;**4**:3865. doi:10.1038/srep03865

[20] Dutta S, Pati SK. Novel properties of graphene nanoribbons: A review. Journal of Materials Chemistry. 2010;**20**(38):8207–23. doi:10.1039/C0JM00261E

[21] Bai J, Cheng R, Xiu F, Liao L, Wang M, Shailos A, et al. Very large magnetoresistance in graphene nanoribbons. Nature Nanotechnology. 2010;**5**(9):655–9. doi:10.1038/nnano.2010.154

[22] Yang L, Cohen ML, Louie SG. Excitonic effects in the optical spectra of graphene nanoribbons. Nano Letters. 2007;**7**(10):3112–5. doi:10.1021/nl0716404

[23] Ni Y, Yao K, Fu H, Gao G, Zhu S, Wang S. Spin seebeck effect and thermal colossal magnetoresistance in graphene nanoribbon heterojunction. Scientific Reports. 2013;**3**:1380. doi:10.1038/srep01380

[24] Xia D, Xue Q, Xie J, Chen H, Lv C, Besenbacher F, et al. Fabrication of carbon nanoscrolls from monolayer graphene. Small. 2010;**6**(18):2010–9. doi:10.1002/smll.201000646

[25] Wang L, Zhang HW, Zhang ZQ, Zheng YG, Wang JB. Buckling behaviors of single-walled carbon nanotubes filled with metal atoms. Applied Physics Letters. 2007;**91**(5):051122. doi:10.1063/1.2767249

[26] Cicero G, Grossman JC, Schwegler E, Gygi F, Galli G. Water confined in nanotubes and between graphene sheets: A first principle study. Journal of the American Chemical Society. 2008;**130**(6):1871–8. doi:10.1021/ja074418+

[27] Sun H. COMPASS: An ab initio force-field optimized for condensed-phase applications overview with details on alkane and benzene compounds. The Journal of Physical Chemistry B. 1998;**102**(38):7338–64. doi:10.1021/jp980939v

[28] Bunte SW, Sun H. Molecular modeling of energetic materials: The parameterization and validation of nitrate esters in the COMPASS force field. The Journal of Physical Chemistry B. 2000;**104**(11):2477–89. doi:10.1021/jp991786u

[29] Wang Q, Duan WH, Liew KM, He XQ. Inelastic buckling of carbon nanotubes. Applied Physics Letters. 2007;**90**(3):033110. doi:10.1063/1.2432235

[30] Wang Q. Atomic transportation via carbon nanotubes. Nano Letters. 2009;**9**(1):245–9. doi:10.1021/nl802829z

[31] Sun H, Mumby SJ, Maple JR, Hagler AT. An ab initio CFF93 all-atom force field for polycarbonates. Journal of the American Chemical Society. 1994;**116**(7):2978–87. doi:10.1021/ja00086a030

[32] Rigby D, Sun H, Eichinger BE. Computer simulations of poly(ethylene oxide): Force field, pvt diagram and cyclization behaviour. Polymer International. 1997;**44**(3):311–30. doi:10.1002/(SICI)1097-0126(199711)44:3<311::AID-PI880>3.0.CO;2-H

[33] Andersen HC. Molecular dynamics simulations at constant pressure and/or temperature. The Journal of Chemical Physics. 1980;**72**(4):2384–93. doi:10.1063/1.439486

[34] Wittung P, Nielsen PE, Buchardt O, Egholm M, Nordén B. DNA-like double helix formed by peptide nucleic acid. Nature. 1994;**368**(6471):561–3. doi:10.1038/368561a0

[35] Brodsky B, Ramshaw JAM. The collagen triple-helix structure. Matrix Biology. 1997;**15**(8–9):545–54. doi:10.1016/S0945-053X(97)90030-5

[36] Bets KV, Yakobson BI. Spontaneous twist and intrinsic instabilities of pristine graphene nanoribbons. Nano Research. 2009;**2**(2):161–6. doi:10.1007/s12274-009-9015-x

[37] Ruoff RS, Tersoff J, Lorents DC, Subramoney S, Chan B. Radial deformation of carbon nanotubes by van der Waals forces. Nature. 1993;**364**(6437):514–6. doi:10.1038/364514a0

[38] Snir Y, Kamien RD. Entropically driven helix formation. Science. 2005;**307**(5712):1067. doi:10.1126/science.1106243

[39] Janiak C. A critical account on [small pi]-[small pi] stacking in metal complexes with aromatic nitrogen-containing ligands. Journal of the Chemical Society, Dalton Transactions. 2000(21):3885–96. doi:10.1039/B003010O

[40] Yan K, Xue Q, Xia D, Chen H, Xie J, Dong M. The core/shell composite nanowires produced by self-scrolling carbon nanotubes onto copper nanowires. ACS Nano. 2009;**3**(8):2235–40. doi:10.1021/nn9005818

[41] Lu W, Chou T-W, Kim B-S. Radial deformation and its related energy variations of single-walled carbon nanotubes. Physical Review B. 2011;**83**(13):134113. doi:10.1103/PhysRevB.83.134113

[42] Li Y, Sun F, Li H. Helical wrapping and insertion of graphene nanoribbon to single-walled carbon nanotube. The Journal of Physical Chemistry C. 2011;**115**(38):18459–67. doi:10.1021/jp205210x

[43] Yan K, Xue Q, Zheng Q, Xia D, Chen H, Xie J. Radial collapse of single-walled carbon nanotubes induced by the Cu_2O surface. The Journal of Physical Chemistry C. 2009;**113**(8):3120–6. doi:10.1021/jp808264d